European Journal of Pharmaceutics and Biopharmaceutics 76 (2010) 95–104

Contents lists available at ScienceDirect

European Journal of Pharmaceutics and Biopharmaceutics

journal homepage: www.elsevier.com/locate/ejpb

Research paper

Forecasting *in vivo* oral absorption and food effect of micronized and nanosized aprepitant formulations in humans

Yasushi Shono [a,1], Ekarat Jantratid [a,2], Filippos Kesisoglou [b], Christos Reppas [c], Jennifer B. Dressman [a,*]

[a] *Institute of Pharmaceutical Technology, Goethe University, Frankfurt am Main, Germany*
[b] *Department of Pharmaceutical Research, Merck & Co. Inc., Pennsylvania USA*
[c] *Faculty of Pharmacy, National and Kapodistrian University of Athens, Athens, Greece*

ARTICLE INFO

Article history:
Received 19 December 2009
Accepted in revised form 25 May 2010
Available online 1 June 2010

Keywords:
Aprepitant
Micronization
Nanosizing
Biorelevant dissolution testing
In silico simulation
Absorption modeling

ABSTRACT

This study coupled results from biorelevant dissolution tests with *in silico* simulation technology to forecast *in vivo* oral absorption of micronized and nanosized aprepitant formulations in the pre- and postprandial states. *In vitro* dissolution tests of the nanosized aprepitant formulation and micronized drug were performed in biorelevant and compendial media. An *in silico* physiologically based pharmacokinetic (PBPK) model was developed based on STELLA® software using dissolution kinetics, standard gastrointestinal (GI) parameters and post-absorptive disposition parameters. GI parameters (gastric emptying rate and GI fluid volume) were varied according to the dosing conditions. Disposition parameters were estimated by fitting compartmental models to the *in vivo* oral PK data. Predictions of *in vivo* performance in each prandial state were evaluated using the AUC and C_{max} generated from the simulated PK profiles. To predict oral absorption from the extremely fast dissolving nanosized aprepitant formulation, several variations on a previously published model were evaluated. Although models that assumed that the formulation behaved as an oral solution or that adjusted the dissolution kinetics according to the different numbers of particles per gram between micronized and nanosized aprepitant generated profiles similar to the observed *in vivo* data in the fed state, simulated profiles for the fasted state showed much faster absorption than that observed in the *in vivo* data. This appeared to result from the assumption of no absorption restrictions in those models. To better predict *in vivo* performance in both fasted and fed states, a model that adds permeability restrictions to absorption was applied. This model not only simulated the *in vivo* profiles for aprepitant well in both prandial states, but also predicted the dependency of the pharmacokinetics on the dose and the particle size of aprepitant. In conclusion, a model based on STELLA® software combined with dissolution results in biorelevant media successfully forecasts the *in vivo* performance of both nanosized and micronized formulations of aprepitant in the fed and fasted states. Although dissolution is the primary limitation to the rate of absorption for micronized aprepitant, some permeability restrictions are revealed for the nanosized formulation. The results also indicate that biorelevant dissolution media have strong advantages over compendial media in forecasting the *in vivo* behavior of aprepitant.

1. Introduction

Aprepitant is a neurokinin 1 (NK1) receptor antagonist that is lipophilic (log *D* at pH 7 = 4.8), poorly soluble (3–7 μg mL^{-1} over the pH range 2–10) and weakly basic [1]. According to the Biopharmaceutics Classification System (BCS) criteria [2,3], aprepitant can be categorized into BCS Class IV, being neither "*highly soluble*" nor "*highly permeable*". Poorly soluble compounds tend to exhibit higher systemic exposure when taken with food, rather than under fasting conditions, due to physiological changes such as prolonged gastric residence, stimulation of bile secretions, increase in available gastrointestinal (GI) fluid volume and, in some cases, interactions with food components [4,5]. Food-effect studies on bioavailability (BA) and fed state bioequivalence (BE) for orally administered solid dosage forms are often conducted by pharmaceutical companies, and the Food and Drug Administration (US FDA) provides guidance to pharmaceutical companies in terms of study design and data analysis of such studies as well as for subsequent product labeling [6].

* Corresponding author. Institute of Pharmaceutical Technology, Goethe University, Max-von-Laue-Str. 9, 60438 Frankfurt am Main, Germany. Tel.: +49 69 798 29680; fax: +49 69 798 29694.
E-mail address: dressman@em.uni-frankfurt.de (J.B. Dressman).
[1] Present Address: CMC Center, Takeda Pharmaceutical Company, Ltd., Osaka, Japan.
[2] Present Address: Department of Pharmacy, Faculty of Pharmacy, Mahidol University, Bangkok, Thailand.

0939-6411/$ - see front matter © 2010 Elsevier B.V. All rights reserved.
doi:10.1016/j.ejpb.2010.05.009

Although drug administration after food ingestion is an effective approach to improve the oral BA of poorly soluble drugs [7,8], it is not always desirable. First, diminishing the differences in systemic exposure between the prandial states will help improve efficiency and safety of medication, as well as patient compliance. Second, for some indications, enhancement of drug absorption in the fasted state is highly desirable e.g. the use of aprepitant for the prevention of chemotherapy-induced nausea and vomiting [1,9]. To achieve these goals, several formulation approaches have been developed for poorly soluble compounds [10], including the use of alternative salt forms [11], crystal engineering (co-crystals and amorphous systems) [12], particle size reduction [13] and lipid formulation [14]. In the case of aprepitant, the Nano-Crystal technology (Elan Corporation, plc, Dublin Ireland) [15], with which drug particles are milled to sub-micron size and stabilized with polymer or surfactant, was selected for the marketed formulation (EMEND®). This nanosized aprepitant formulation was able to overcome non-linear pharmacokinetics in the fasted state and reduce the positive food effect observed with the micronized formulation within the clinical dose range [1]. Nanosizing technology has also been applied to reduce variability in pharmacokinetic behavior of oral dosage forms e.g. for TriCor® (fenofibrate) [16] and Rapamune® (Sirolimus).

At the preformulation stage, prediction of food effects is important to developing oral formulations with the desired bioperformance [17]. The BCS [4], the Biopharmaceutical Drug Disposition Classification System (BDDCS) [18] and other statistical models [19] based upon physical chemical properties of drug can roughly classify drugs into three categories (positive, negative or no food effects), but it is still a challenge to predict food effects quantitatively. Since formulation effects on dissolution kinetics can also affect intestinal absorption of the drug, *in vitro* dissolution testing using biorelevant media is a useful tool to predict *in vivo* performance of drug products, including food effects [20–22]. Another approach to prediction of the *in vivo* performance is *in silico* physiologically based pharmacokinetic (PBPK) modeling, using software packages such as GastroPlus®, PK-Sim®, and STELLA® [23–25]. These *in silico* techniques use physiological parameters together with available/predicted *in vitro* data for the drug (solubility, dissolution, permeability, metabolism and disposition of the drug) to simulate the plasma profiles.

Nicolaides et al. demonstrated the use of a simple integrated model using STELLA® software to predict *in vivo* performance of diverse lipophilic compounds such as atovaquone and troglitazone using biorelevant dissolution data [26,27]. In a recent study, it was shown that prediction of food effects based solely upon the extent of dissolution in biorelevant media in the USP paddle assembly was not appropriate for celecoxib. Although sink conditions are generated *in vivo* by the very high permeability of celecoxib [28], the dissolution in the limited volume available in the paddle apparatus created non-sink conditions. However, by coupling the *in vitro* biorelevant dissolution data with *in silico* simulation using STELLA® software using the Nicolaides et al. model, the *in vivo* performance of celecoxib in both prandial states was simulated well [29]. The next challenge is to apply the *in vitro–in silico–in vivo* (IVISIV) method to quantitatively predict the *in vivo* performance of poorly soluble drugs formulated in special technologies, such as nanosized formulations.

In this study, we selected aprepitant as a model compound. The marketed formulation of aprepitant uses nanosizing technology to improve oral BA and minimize food effects. Data were also available for a development formulation containing micronized aprepitant. Specifically, the aims of this study were to: (1) forecast *in vivo* oral absorption of aprepitant and its formulation effects in the fasted and fed states, applying the *in vitro* biorelevant dissolution testing coupled with *in silico* PBPK modeling using the STELLA® software, (2) simulate the dose- and particle size-dependent food effect of aprepitant, and (3) investigate the advantages of using biorelevant media over simple buffer media for predicting *in vivo* performance of the nanosized aprepitant formulation.

2. Materials and methods

2.1. Chemicals and reagents

Granules of the nanosized aprepitant formulation and micronized drug substance (mean particle size: 120 nm and 7 μm, respectively) were provided by Merck & Co., Inc. (West Point, PA, USA). Long-life, heat-treated and homogenized milk (UHT milk) containing 3.5% fat (Milfina Hochwald, Kaiserslautern, Germany) was purchased commercially. Glyceryl monooleate (GMO, Rylo M19 Pharma®, 99.5% monoglyceride, lot 173,403-2202/107) was kindly donated by Danisco Specialities, Brabrand, Denmark. Egg phosphatidylcholine (Lipoid E PC®, 99.1% pure, lot 108015-1/42) was a kind donation from Lipoid GmbH, Ludwigshafen, Germany. 85% orthophosphoric acid (H_3PO_4), 37% hydrochloric acid (conc. HCl) and pepsin (Ph. Eur., 0.51 U/mg, lot 1241256) were obtained from Fluka Chemie AG, Buchs, Switzerland. Maleic acid (99% pure, lot 4039128) was purchased from Sigma–Aldrich Chemie GmbH, Steinheim, Germany. Sodium oleate (82.7% pure, lot 51110) was obtained from Riedel-de Haën, Seelze, Germany. Sodium taurocholate (NaTC, 97% pure, lot 2007100274) was purchased from Prodotti Chimici e Alimentari SpA, Basaluzzo, Italy. Sodium hydroxide solution (0.1 N NaOH) and hydrochloric acid solution (0.1 N HCl) were purchased from VWR International GmbH, Darmstadt, Germany. Dichloromethane, acetonitrile, glacial acetic acid, sodium acetate trihydrate, sodium chloride (NaCl), potassium dihydrogen phosphate and NaOH pellets were all of analytical grade and purchased from Merck KGaA, Darmstadt, Germany.

2.2. Media preparation

The compositions and the preparation procedures of the media used for dissolution tests and solubility determination have been described previously [30–32]. Fasted State Simulated Gastric Fluid (FaSSGF) [31], Fed State Simulated Gastric Fluid (FeSSGF) [32] and compendial Simulated Gastric Fluid without pepsin (SGF_{sp}) (USP 32) were used for the gastric media. For the upper small intestine, updated versions of Fasted State Simulated Intestinal Fluid (FaSSIF-V2) and Fed State Simulated Intestinal Fluid (FeSSIF-V2) [32] and compendial Simulated Intestinal Fluid without pancreatin (SIF_{sp}) (USP 32) were also used in this study.

2.3. Analytical methods

2.3.1. The high-performance liquid chromatography (HPLC) system

The samples obtained from solubility and dissolution tests were quantitatively analyzed for aprepitant concentration using an isocratic HPLC system. The HPLC system consisted of a pump (Merck Hitachi L7100), an autosampler (Merck Hitachi L-7200) and a UV detector (Merck Hitachi L-7400). The chromatograms were evaluated with EZChrom Elite™ Version 2.8 Software (Biochrom Ltd., Cambridge, UK). The analytical column used was a Zorbax Rx-C8 4.6 mm i.d. × 150 mm, 5 μm from Agilent Technologies (Waldbronn, Germany). The mobile phase was a mixture of acetonitrile and 0.1% H_3PO_4 solution (50:50) at a flow rate of 1.5 mL min^{-1}. The injection volume was 50 μL. The detection wavelength was set at 220 nm. The analysis was performed under ambient conditions.

2.4. Solubility measurements

The shake-flask method was employed for aprepitant solubility determination in all media, using micronized drug. Measurement was performed by adding an excess amount of the drug substance to a medium in a glass vial. The vial was incubated in a water bath at 37 °C and shaken vigorously at appropriate intervals. Samples were taken after at least 6 h and filtered through polyvinylidene fluoride (PVDF) membrane filters with a pore size of 0.45 μm (Whatman GmbH, Dassel, Germany). The filtrate was diluted immediately with mobile phase and then analyzed by HPLC. For FeSSGF, with milk as a major component, the use of filters with a small pore size was not possible. Glass syringe filters with a pore size of 2.7 μm (25 mm GD/X, Whatman) were used to separate non-dissolved drug from the samples. Then, 1 mL of acetonitrile was added to 0.5 mL of the filtrate and mixed well, and the mixture was centrifuged at 7500 rpm for 3 min. The supernatant was analyzed by HPLC.

2.5. Dissolution testing of nanosized aprepitant formulation and micronized drug

2.5.1. USP apparatus II (paddle assembly)

The dissolution conditions consisted of a medium volume of 500 mL per vessel with a paddle revolution speed of 50 rpm. The sampling times were 5, 10, 15, 20, (25), 30, 45 and 60 min for micronized drug and 1, 2, 3, 5, 7.5 and 10 min for the nanosized formulation. The temperature in the vessels was maintained at 37 °C ± 0.5 °C throughout each dissolution run. Experiments were conducted at least in triplicate. Accurately weighed samples corresponding to 125 mg aprepitant were transferred into glass tubes, 2.5 mL of water was added, and the tube was gently swirled to disperse the particles. The resulting suspension was transferred into the dissolution vessel. At the above-mentioned times, samples were withdrawn through cylindrical polyethylene filter sticks having a pore size of 10 μm and fitted directly on the end of sampling devices. The volume withdrawn was approximately 5 mL for each sampling time point. The samples to be tested for micronized aprepitant were then filtered through a 0.45-μm PVDF filter (Whatman GmbH, Dassel, Germany) into the test tubes, after discarding the first 2 mL. Because the particle size of the drug in the nanosized formulation is approximately 120 nm, the samples were filtered through a 0.1-μm Anotop 25 plus (Whatman GmbH, Dassel, Germany). After discarding the first 2 mL, the filtrate was collected and assayed. Pretreatment for FeSSGF samples was performed by the same procedure described for the solubility measurements. Since the particle size of the drug in nanosized formulation is much smaller than the lowest pore size (2.7 μm) membrane filter that can be used for FeSSGF, only the micronized aprepitant was tested in that medium.

2.5.2. Mini-paddle assembly

To simulate the volume availability in the fasted stomach, the mini-paddle apparatus was applied for dissolution testing in FaSSGF and SGF_{sp}. The mini-paddle apparatus is based on the USP paddle setup but scaled down geometrically with respect to the dimensions [33], so that hydrodynamics remain essentially similar at a given rpm. The dissolution conditions consisted of a medium volume of 250 mL per vessel with a paddle revolution speed of 50 rpm.

2.6. Available pharmacokinetic data and assessments

The plasma drug concentration–time profiles after oral administration of nanosized aprepitant formulation were taken from the literature [34]. In this clinical study, 20 healthy adult subjects (nine women and 11 men) were administered the marketed capsule formulation containing 125 mg aprepitant, either under fasting conditions or within fifteen minutes of ingesting a standard breakfast, in a single dose, randomized crossover study. Each dose was administered with 8 fl. Oz. of water. Plasma drug concentrations were estimated directly from the profile. Pharmacokinetic analysis was performed using WinNonlin® Professional Edition 5.2 software (Pharsight Corporation, Mountain View, CA, USA). Since no appropriate intravenous administration data were available, post-absorptive disposition parameters needed for the simulation were estimated by fitting for *in vivo* mean plasma concentration–time curves after oral administration based on an oral one-compartment model (WinNonlin® Model-4) as shown in Table 1. Observed and simulated plasma aprepitant concentration–time profiles were analyzed for the following pharmacokinetic parameters based on non-compartmental analysis: area under the plasma concentration–time curve (AUC), the peak plasma concentration (C_{max}) and the time to reach C_{max} (T_{max}).

2.7. Computer simulation of the plasma profile for aprepitant

The plasma profiles for aprepitant were simulated using the STELLA® 9.0 software (Cognitus Ltd., North Yorkshire, UK). Fig. 1 shows the basic model structure used for *in silico* simulation. Four model structures, the first of which is the same as that published previously [27,29], were developed to predict *in vivo* performance of aprepitant. This model assumes negligible absorption from the stomach, simultaneous solid and liquid emptying from the stomach and no intestinal permeability restrictions. First-order gastric emptying rate in the fasted state at 2.8 h^{-1} and zero-order gastric emptying rate in the fed state at 4 kcal min^{-1} were taken from average population values [35]. The amount of drug entering the plasma, i.e., contributions from dissolved drug emptied from the stomach and drug dissolved in the small intestine, was translated into plasma concentration using the ratio of the volume of distribution to the fraction absorbed (Vd/*F*), which is estimated with WinNonlin® directly from the oral administration data.

To calculate *in vivo* dissolution in the model, the *in vitro* dissolution parameters were incorporated into the model by applying a modification of the Noyes–Whitney equation [20]. This equation is based on the assumption of isometric, similarly sized particles with continuously decreasing surface area (due to ongoing dissolution). The ratio D/δ, where D is the diffusion coefficient and δ is the diffusion layer thickness, is assumed to remain constant during the dissolution process. The dissolution rate is thus given by the following Eq. (1):

$$\frac{dW_t}{dt} = \frac{D\Gamma N^{1/3}}{V\delta\rho^{2/3}} W^{2/3}(X_s - W_t) = zW^{2/3}(C_s - C) \quad (1)$$

where W_t is the amount of drug dissolved at time t, W the amount of drug remaining to be dissolved, X_s the amount of drug that saturates the volume V of the dissolution medium, C_s the solubility of drug, C the concentration of the dissolved drug at time t, ρ the particle density, Γ the shape factor, N the number of particles to be dissolved

Table 1
Values of correlation coefficients for the profiles of best fit to the mean observed plasma data, after oral administration of nanosized aprepitant formulation 125 mg in the fasted and fed states, and disposition parameters estimated with WinNonlin®, assuming one-compartment disposition kinetics[a].

	Correlation coefficient	Vd/*F* (L)	K_{10} (h^{-1})
Fasted	0.983	138.0	0.041
Fed	0.982	104.5	0.041

[a] Vd, apparent volume of distribution; *F*, bioavailability coefficient; K_{10}, elimination rate constant.

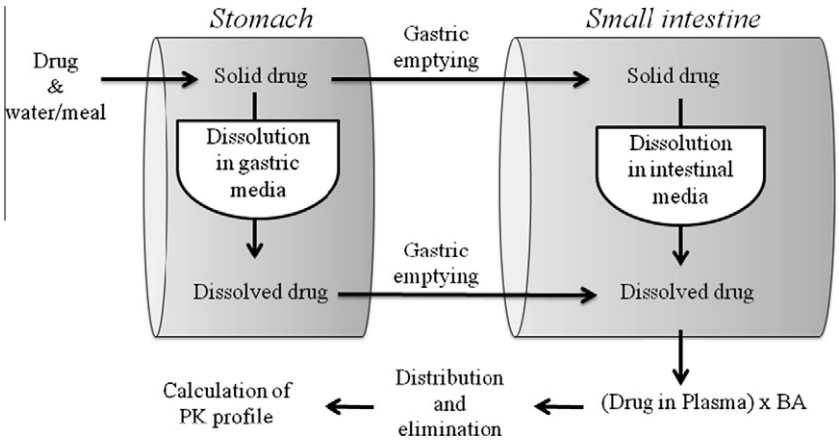

Fig. 1. Basic model structure to simulate pharmacokinetic profiles.

and z is the dissolution parameter, which is a constant equal to $D\Gamma N^{1/3}/\delta\rho^{2/3}$. Whereas sink conditions were assumed to prevail in the small intestine, dissolution in the stomach was assumed to occur until the drug concentration reached its solubility (since it is reasonable to argue that there is no quantitative absorption of aprepitant from the stomach).

Four simulation models were investigated:

Model-1: This was the same model that had been used for celecoxib in a previous paper [29]. Since the dissolution rate from the nanosized formulation was extremely high, reaching a plateau within 2 min, it was impossible to estimate the z values directly from the dissolution profiles. Therefore, it was necessary to develop further models.

Model-2: This model assumes the administered formulation to be essentially a solution. In this model, administered drug moves into the small intestine in accordance with the gastric emptying rate and then migrates immediately into plasma. Like Model-1, this model also assumes that there is no permeability restriction to intestinal uptake.

Model-3: This model is structured the same way as Model-1, with the exception that the z value of the nanosized formulation was estimated according to the number of particles per dose in the micronized (7 μm) and nanosized (0.12 μm) aprepitant, as an alternative to measuring the dissolution profile of the nanosized preparation. The corresponding z values for different particle sized drug were estimated by the following Eq. (2):

$$\frac{z_{\text{micronized}}}{z_{\text{nanosized}}} = \frac{N^{1/3}_{\text{micronized}}}{N^{1/3}_{\text{nanosized}}} \quad (2)$$

where $N_{\text{micronized}}$ and $N_{\text{nanosized}}$ is a relative number of particles of micronized and nanosized aprepitant, respectively. A factor of 58.3 for the z value ratio was estimated in accordance with Eq. (2).

Model-4: In addition to the features described above for Model-3, Model-4 incorporates a restriction into the permeation process. Mathematically, restrictions based on diffusion of drug through the unstirred water layer (UWL) vs. an overall reduction in membrane permeability cannot be distinguished. Takano et al. successfully applied an integrated model using STELLA® software incorporating a membrane permeation limited by the diffusion through the UWL to predict intestinal absorption and its rate-limiting steps for diverse lipophilic compounds [36,37] with log D of 0.7–6.5 and Caco-2 permeability of 2.7–10.1 $\times 10^{-5}$ cm s^{-1}. Alternatively, for drugs with less than optimal permeability, such as aprepitant, an adjustment in the uptake rate constant can be made. This adjustment should be based on permeability comparison with substances of known fraction absorbed and preferably having no solubility restrictions to absorption e.g. metoprolol and mannitol. In the case of aprepitant, the permeability (P_{app} = 7.8 $\times 10^{-6}$ cm s^{-1}) was calculated from appropriate Caco-2 cell data. In the same experimental setup, metoprolol (high permeability reference compound) was determined to have a permeability of P_{app} = 16.1 $\times$ 10^{-6} cm s^{-1} and mannitol (low permeability reference compound) a permeability of $P_{\text{app}} < 1 \times 10^{-6}$ cm s^{-1} [1].

In all models, the basal intestinal fluid volume was set at 100 mL and 250 mL in the fasted and fed state, respectively, based upon the average value in the literature [38,39]. Volumes representing any co-administered water and/or meal (240 mL water for the fasted state and 750 mL for the total meal volume in the fed state) were added to the basal volumes to reflect amounts ingested in the corresponding pharmacokinetic studies. To estimate the effective intestinal surface area, the intestinal surface area and volume ratio was set at 2.25, which is within the range reported in the literature (1.33–4.16) [39–41] and can be regarded as a reasonable value to simulate *in vivo* profiles based on sensitivity analyses. Although intestinal transit time is known to be similar in both prandial states, approximately 4 h [22], gastric emptying time in the fed state is controlled by the number of calories of food ingested. From these considerations, the dissolution process in the small intestine was terminated in the simulations after 4 h and 6 h in the fasted and fed state, respectively. Disposition parameters (Vd/F and K_{10}) estimated from the observed data after oral administration in the fed state were used for the simulations in both prandial states, as there is no reason to assume that these are affected by food intake.

3. Results and discussion

3.1. Solubility of aprepitant in biorelevant and compendial media

Equilibrium solubility of micronized aprepitant in biorelevant and compendial media at 37 °C is shown in Table 2. Aprepitant is not only a poorly soluble according to the BCS criteria, but also exhibits pH-dependent solubility at pH below 2. The solubility of aprepitant in SGF_{sp} (pH 1.2) and FaSSGF (pH 1.6) was much higher than in SIF_{sp} (pH 6.8), in line with a previous report [1]. In spite of the more neutral pH, solubility in FeSSGF (pH 5.0) was higher than in FaSSGF indicating that aprepitant may be incorporated into the casein micelles present in the milk-containing FeSSGF. FaSSIF-V2 and FeSSIF-V2 enhanced the drug solubility, mainly due to the mixed-micelle effects. Differences in solubility between FaSSIF-V2 and FeSSIF-V2 indicate that food has the potential to exhibit a positive effect on absorption of aprepitant.

Table 2
Summary of solubility data and *z* values of aprepitant in biorelevant and compendial media at 37 °C.

Medium	Solubility (mg mL^{-1})		*z* value[c] (mL mg$^{-2/3}$ h^{-1})
	Micronized[a]	Nanosized[b]	
SGF_{sp}	0.0206	0.0391	0.2955
FaSSGF	0.0066	0.0166	0.2768
FeSSGF	0.0091	n.a.	0.0624
SIF_{sp}	0.0007	0.0013	0.0488
FaSSIF-V2	0.0054	0.0136	0.1961
FeSSIF-V2	0.0924	0.1018	0.2187

n.a. not assessed.
[a] Solubility measured with micronized aprepitant.
[b] Maximum concentration in the vessel after completion of dissolution of nanosized aprepitant formulation.
[c] Estimated for micronized aprepitant.

3.2. Dissolution of aprepitant in biorelevant and compendial media

Fig. 2a and b shows the dissolution profiles of aprepitant in the simulated gastric media. The average maximum percentage release of micronized aprepitant in FaSSGF and SGF_{sp} (control), which are used to simulate the preprandial gastric conditions, was 1.7% and 5.7%, respectively; these results were in good agreement with the solubility data. In FeSSGF, micronized aprepitant exhibited a lower extent of release than in other gastric media. As shown in Fig. 2c, dissolution profiles of micronized aprepitant in FaSSIF-V2 and FeSSIF-V2 were significantly different from each other, showing average maximum percentage dissolved of 1.9% and 35.7%, respectively, whereas dissolution in SIF_{sp} was negligible. This is a typical pattern for dissolution of drugs with positive food effects, e.g., atovaquone, troglitazone [26,42]. When aprepitant 100-mg tablets containing micronized drug were given to humans together with a standard breakfast, a significant increase in AUC (about threefold) was observed compared to administration in the fasted state [1]. Likewise, a suspension made with conventional micronized aprepitant (mean particle size of 5.5 μm) given to Beagle dogs in the fed state exhibited a significant increase in AUC (3.2-fold) and C_{max} (2.3-fold) compared to the fasted state [1]. The prediction of food effects based solely on the extent of dissolution in FaSSIF-V2 and FeSSIF-V2 overestimates the *in vivo* results. This result is similar to that observed in our previous case example of celecoxib [29].

As shown in Fig. 2b and d, dissolution profiles of nanosized aprepitant formulation in all media tested reached a plateau level within the first or second sampling time point (1 or 2 min). It is clear that nanosizing the formulation of aprepitant results in almost instant dissolution and can thus be a powerful driving force to improve the BA of aprepitant. Indeed, the nanosized formulation was able to almost completely eliminate the food effect seen with the micronized formulation [34]. In addition to dissolution rate enhancement, the extent of dissolution was higher for the nanosized formulation than for the micronized drug. An increase in the saturation solubility with decreasing particle size according to the Ostwald–Freundlich equation is expected to contribute to dissolution rate enhancement [43]. Theoretically, reducing particle size of micronized substance to sub-micron range would lead to an

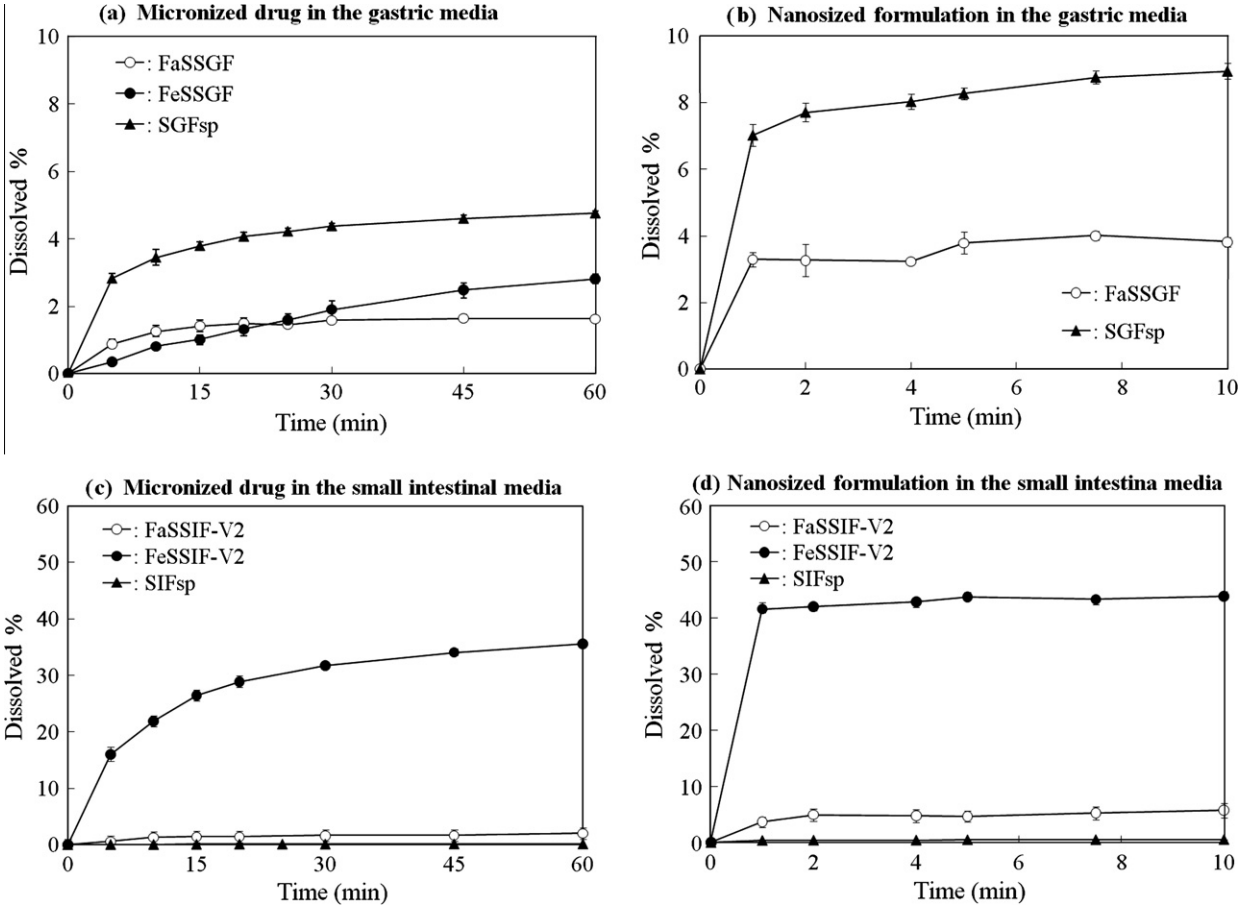

Fig. 2. Dissolution profiles of 125 mg aprepitant micronized drug and nanosized formulation in the gastric and the small intestinal media: (a) micronized drug in the gastric media, (b) nanosized formulation in the gastric media, (c) micronized drug in the small intestinal media, and (d) nanosized formulation in the small intestinal media. All results are shown as "mean% dissolved ± s.d.".

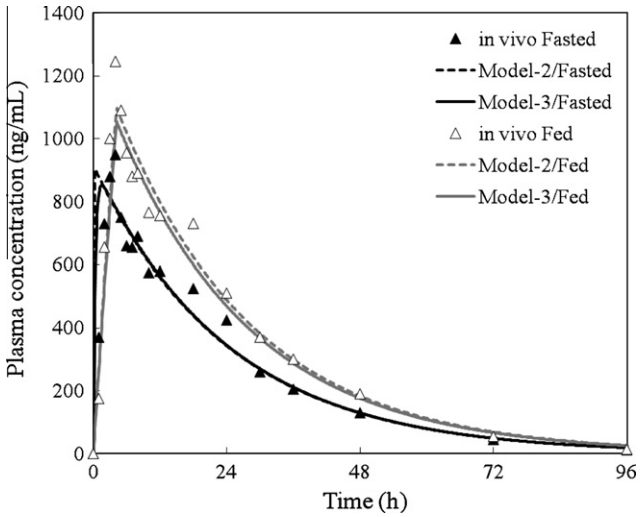

Fig. 3. Simulated plasma profiles of aprepitant 125 mg nanosized formulation in the fasted and fed states using Model-2 and Model-3.

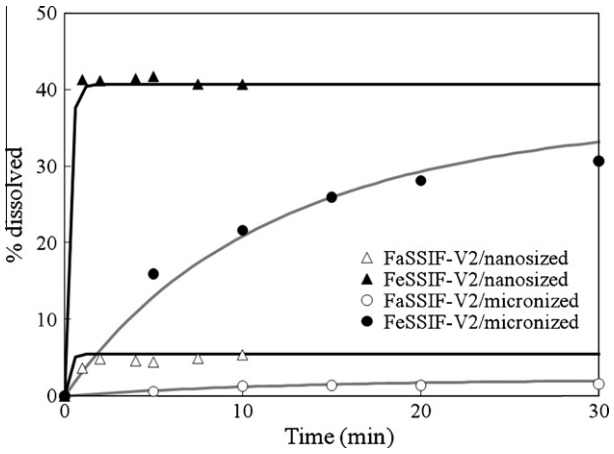

Fig. 4. Dissolution data and corresponding simulated dissolution profiles for nanosized formulation and micronized aprepitant in FaSSIF-V2 and FeSSIF-V2.

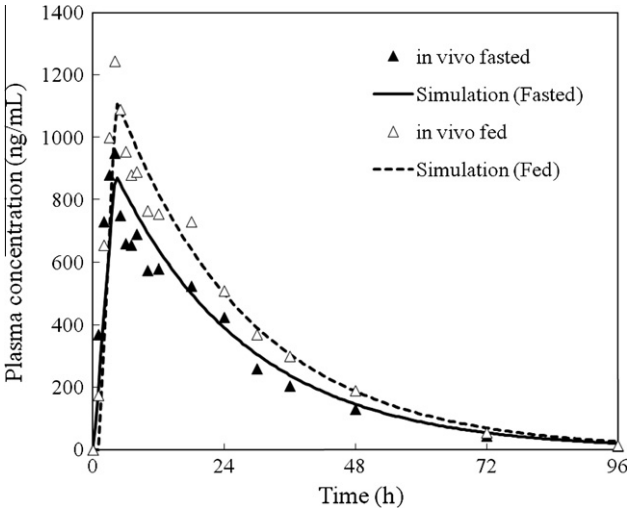

Fig. 5. Simulated plasma profiles of nanosized aprepitant formulation 125 mg in the fasted and fed states using Model-4.

Table 3
Pharmacokinetic parameters estimated from the simulated plasma profiles of the nanosized aprepitant formulation generated with various STELLA® models vs. mean data observed in pharmacokinetic studies.

	Fasted state			Fed state		
	T_{max} (h)	C_{max} (ng mL^{-1})	AUC_{0-96} (ng h mL^{-1})	T_{max} (h)	C_{max} (ng mL^{-1})	AUC_{0-96} (ng h mL^{-1})
In vivo	4.0	950	22,169	4.0	1245	29,153
Model-2	0.3	902	21,732	4.2	1098	28,547
Model-3	1.5	851	21,653	4.2	1055	27,422
Model-4	4.5	871	22,898	4.5	1106	28,585

approximate of 10–15% increase in solubility based on the Ostwald–Freundlich equation [13]. Although increases in solubility of up to 50% have been observed for certain compounds, the degree of enhancement possible by nanosizing seems to be still somewhat controversial [43–46]. On the other hand, the higher than expected increase in the maximum concentration measured might be due to incomplete separation of non-dissolved, but very small (<100 nm) drug particles during filtration of samples. For aprepitant, the extent of dissolution *in vitro* appears to have been generally limited by its solubility and by the limited volume of media available in the (mini-)paddle apparatus.

3.3. Simulation of the plasma profiles using STELLA® software

In a previous report, we successfully applied *in silico* modeling to the quantitative prediction of food effects for micronized celecoxib [29]. In the case of nanosized aprepitant, it was impossible to estimate the *z* values directly from the dissolution profiles due to the extremely fast dissolution rate, so the model used for micronized celecoxib (Model-1) could not be applied.

Simulated profiles generated from Model-2 and Model-3 in the fasted (a combination of FaSSGF and FaSSIF-V2) and fed states (a combination of FeSSGF and FeSSIF-V2) are shown in Fig. 3, and the pharmacokinetic parameters estimated from the simulated profiles are summarized in Table 3. In the *fasted* state, the predicted T_{max} obtained from Model-2 was much earlier than the actual *in vivo* data. This is likely due to the assumption that the nanosized aprepitant behaves like an oral solution. Although Model-3 predicted the *in vivo* behavior of nanosized aprepitant better, the absorption rate was still overpredicted. Fig. 4 compares actual

Table 4
Summary of sensitivity analysis for the parameters used in STELLA® Model-4.

Parameter	Fasted state		Fed state	
	Values used (range of values tested)	Effect on simulated plasma profiles	Values used (range of values tested)	Effect on simulated plasma profiles
Gastric emptying rate	2.8 h^{-1} (1.4–5.6)	None	4 kcal min^{-1} (3–5)	None
Solubility in the gastric fluid	0.0166 mg mL^{-1} (0.0083–0.0332)	None	0.0091 mg mL^{-1} (0.00455–0.0182)	None
Solubility in the intestinal fluid	0.0136 mg mL^{-1} (0.0068–0.0272)	Significant	0.1018 mg mL^{-1} (0.0509–0.2036)	None
Basal intestinal fluid volume	100 mL (50–150 mL)	Moderate	250 mL (150–350)	None
Intestinal surface area/volume ratio	2.25 (1.33–4.16)	Significant	2.25 (1.33–4.16)	None

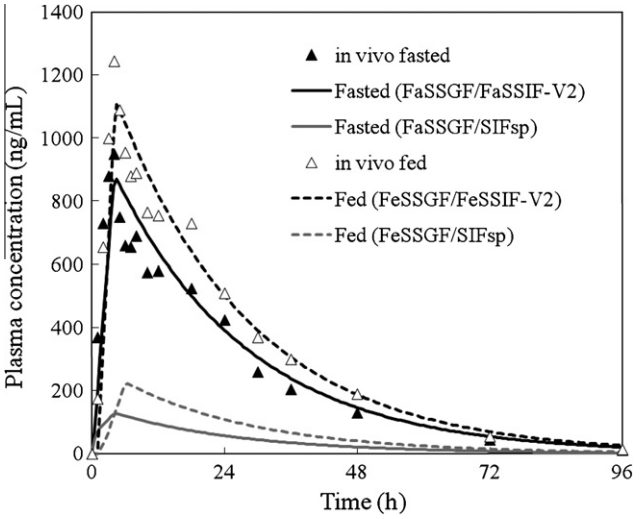

Fig. 6. Simulated plasma profiles of nanosized aprepitant formulation 125 mg in the fasted and fed states using Model-4: comparison of dissolution data from biorelevant and compendial media.

dissolution profiles for the nanosized and micronized aprepitant in the intestinal media along with the curves calculated from the z values according to Eq. (2). Since calculated and observed profiles were consistent, it can be assumed that the z value calculation was not the cause of discrepancies between simulated plasma profiles using Model-3 and the observed plasma profiles (Fig. 3). Instead, it was hypothesized that the overprediction of profiles by Model-2 and Model-3 results from the assumption in these models that there are no intestinal absorption restrictions.

In the *fed* state, by contrast, the simulated profiles generated from both models (Model-2 and Model-3) were similar to each other and fit the *in vivo* profiles well, with the AUC, C_{max} and T_{max} all in good agreement with the *in vivo* data. It appears that intestinal absorption of aprepitant from the nanosized formulation is governed primarily by the gastric emptying in the fed state, consistent with the previous case example of celecoxib [29]. However, when the compendial intestinal medium, SIF_{sp}, was used for the simulations instead of FaSSIF-V2 or FeSSIF-V2, the simulated profiles generated with Model-2 or *Model-3* showed longer T_{max} and a distinct decrease in the C_{max} (simulations not shown), indicating that a certain level of dissolution in the intestine is also required to facilitate absorption.

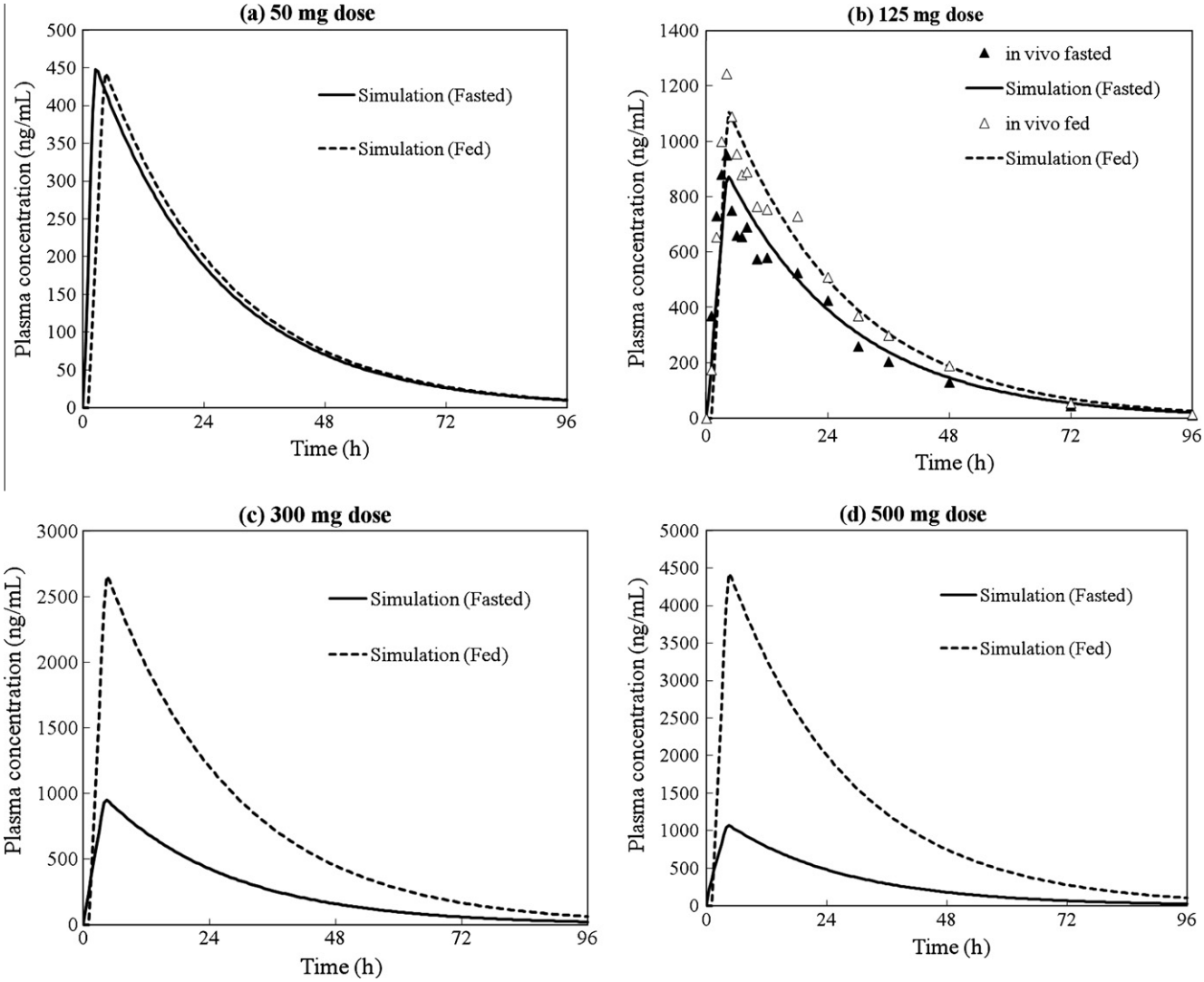

Fig. 7. Simulated plasma profiles generated for various doses of nanosized aprepitant formulation using Model-4. (a) 50 mg dose, (b) 125 mg dose, (c) 300 mg dose, and (d) 500 mg dose.

Simulated plasma profiles in both prandial states generated with Model-4, which invokes a permeability restriction as well as adjusting the *z* values for the particle size, fit the *in vivo* data well. In particular, the T_{max} values are more consistent with the *in vivo* data than in the simulations generated from the other three models, as shown in Fig. 5. All estimated parameters were in good agreement with the *in vivo* data, with point estimates of AUC of 1.03 in the fasted state and 0.98 in the fed state. Similarly, point estimates from the simulations of C_{max} were 0.92 in the fasted and 0.89 in the fed state.

In order to assess the impact of physiological model parameters on the profiles simulated with Model-4, sensitivity analysis was performed for all parameters as summarized in Table 4. Solubility of aprepitant in the intestinal fluid (FaSSIF-V2) was the most crucial parameter influencing the simulated profile in the fasted state, ranging from 52% to 121% in C_{max}. As FaSSIF-V2 was developed based on population values, this result implies an individual variability of PK profile, depending upon individual physiological conditions. Basal intestinal fluid volume affected the fasted profiles moderately within the range explored (50–150 mL) but had no significant impact on the profiles in the fed state (Table 4). Variation of the ratio of intestinal surface area to volume (within the range reported in the literature [39,41,47]) also affected the simulated profiles in the fasted state, depending on the value (Table 4) C_{max} ranged from 61% to 124%. However, variation of surface area to volume ratio did not affect the simulated plasma profile in the fed state. Other parameters did not significantly affect the simulated profiles in either fasted or fed state within the physiologically range explored.

3.3.1. Biorelevant or compendial media?

As shown in Fig. 6, when SIF_{sp} was used instead of biorelevant media to simulate intestinal events, profiles generated from Model-4 predicted much lower systemic exposure in both prandial states. When SGF_{sp} instead of the biorelevant gastric media was used for the simulation in the fasted and fed states, no significant change was observed in the simulation profiles in either case (data not shown). These results indicate that the ability to match aprepitant plasma profiles in the simulations is highly dependent upon the choice of medium to represent the fluids in the small intestine.

3.3.2. Influence of the administered dose on food effects

To evaluate the dose-dependent performance of the nanosized aprepitant formulation, the pharmacokinetic profiles at various doses were simulated using Model-4 (Fig. 7 and Table 5). The AUC simulated at 300-mg dose in the fed state was 2.7-fold higher than under the fasting conditions and hence consistent with the *in vivo* data (2.7-fold) (1). By contrast, the *in vivo* data show only a 1.2-fold increase in the AUC between prandial states for the 125-mg dose. This ratio was also predicted well by the simulations. In addition to good prediction of the escalation of the positive food effect with increasing dose, the simulations also indicate that this phenomenon is primarily due to the exacerbation of solubility limitations in the fasted state.

3.3.3. Effect of particle size of aprepitant on food effect

To evaluate the effects of particle size of the drug in the formulation on the *fed vs. fasted state* performance, simulated plasma profiles were generated for 125 mg aprepitant with various particle sizes (0.12–7 μm) using Model-4. Pharmacokinetic parameters estimated from the simulated profiles of 125 mg aprepitant with different particle sizes are shown in Table 6. Simulated plasma profiles of aprepitant having various particle sizes in the fasted and fed states are shown in Fig. 8. Predicted food effects for micronized drug with a particle size of 7 μm and nanosized formulation are in accordance with the observed *in vivo* results. These results imply that enhancement of dissolution rate by particle size reduction from 7 μm to 0.5 μm diminishes food effect on absorption of aprepitant, but further size reduction to less than 0.5 μm has no additional effect.

Simulated plasma aprepitant profiles and dependency of the food effect on dose and particle size were in good agreement with

Table 5
Pharmacokinetic parameters estimated from the simulated plasma profiles for various doses of the nanosized aprepitant formulation using STELLA® Model-4 vs. the mean values observed after administration of 125 mg.

Dose (mg)	Fasted state			Fed state			Ratio (fed/fasted)	
	T_{max} (h)	C_{max} (ng mL^{-1})	AUC_{0-96} (ng h mL^{-1})	T_{max} (h)	C_{max} (ng mL^{-1})	AUC_{0-96} (ng h mL^{-1})	C_{max}	AUC_{0-96}
Observed								
125 mg	4.0	950	22,169	4.0	1245	29,153	1.3	1.3
Simulated								
50 mg	2.5	448	11,426	4.5	442	11,430	1.0	1.0
125 mg	4.5	871	22,898	4.5	1106	28,585	1.3	1.2
300 mg	4.5	949	25,029	4.5	2655	68,625	2.8	2.7
500 mg	4.5	1068	28,340	4.5	4425	114,338	4.1	4.0

Table 6
Pharmacokinetic parameters estimated from the simulated plasma profiles generated for a dose of 125 mg nanosized aprepitant having various particle sizes and using STELLA® Model-4 vs. the mean observed values.

Particle size (μm)	Fasted state			Fed state			Ratio (fed/fasted)	
	T_{max} (h)	C_{max} (ng mL^{-1})	AUC_{0-96} (ng h mL^{-1})	T_{max} (h)	C_{max} (ng mL^{-1})	AUC_{0-96} (ng h mL^{-1})	C_{max}	AUC_{0-96}
Observed								
0.12	4.0	950	22,169	4.0	1245	29,153	1.3	1.3
Simulated								
0.12	4.5	871	22,898	4.5	1106	28,585	1.3	1.2
0.5	4.5	815	21,436	4.5	1104	28,542	1.4	1.3
2.0	4.5	677	17,811	4.5	1104	28,530	1.6	1.6
7.0	4.5	457	12,041	5.0	1098	28,528	2.4	2.4

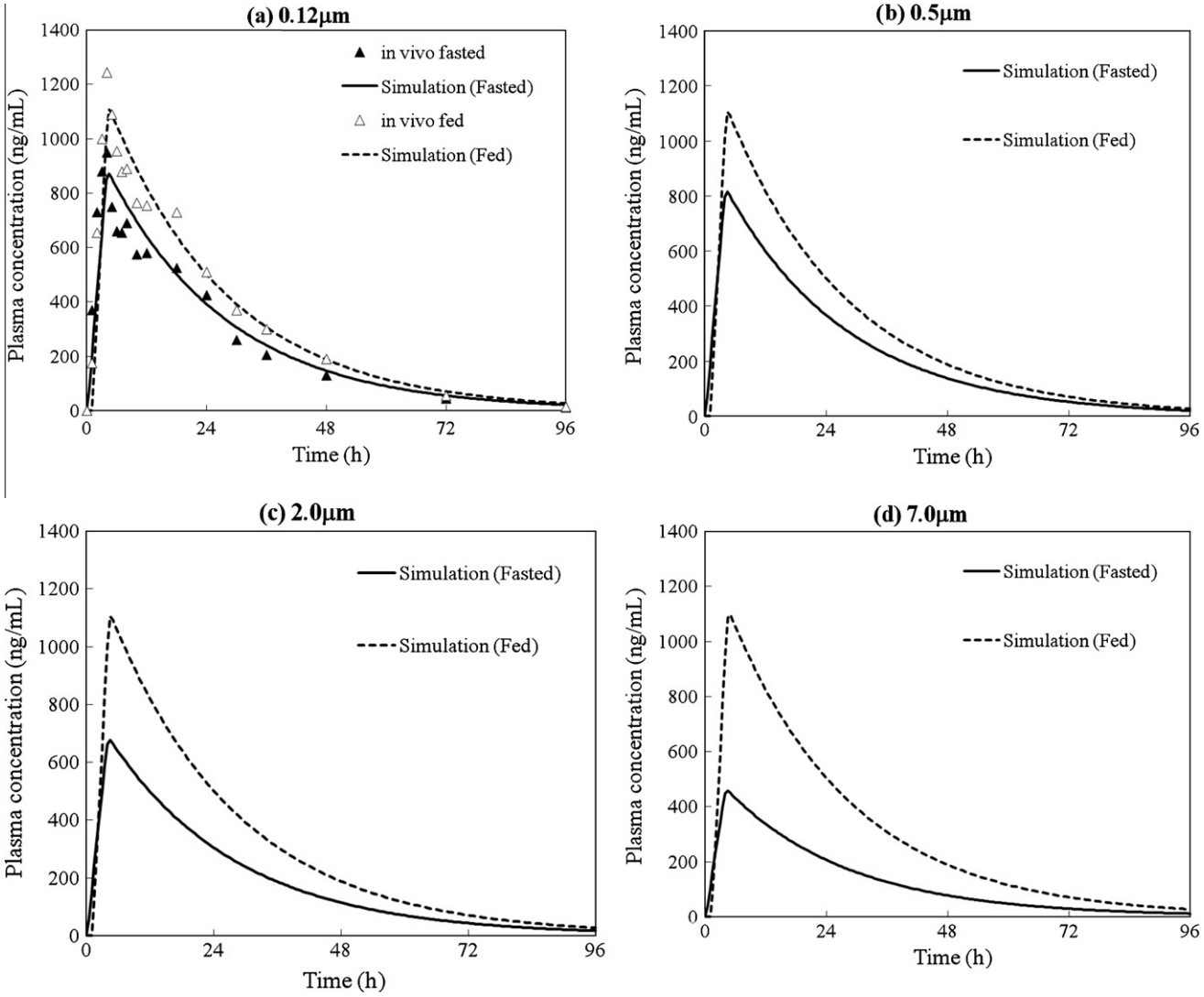

Fig. 8. Simulated plasma profiles generated for various particle sizes of aprepitant using Model-4. (a) 0.12 μm, (b) 0.5 μm, (c) 2.0 μm, and (d) 7.0 μm.

the available *in vivo* data in humans. Furthermore, the results show that *in vitro* dissolution data set using updated biorelevant media [32], which are based upon recent analysis of human GI fluid composition [48], leads to better prediction of *in vivo* performance of aprepitant than standard compendial media.

4. Conclusion

This study indicates that dissolution testing in biorelevant gastric and small intestinal media, coupled with *in silico* STELLA® simulation software, can forecast plasma profiles of aprepitant in either micronized or nanosized form. Additionally, the simulated plasma profiles generated from biorelevant media combinations show a clear advantage over the compendial media in predicting the *in vivo* performance of aprepitant. *In vitro–in silico–in vivo* relationships (IVISIV-R) with Model-4 and biorelevant media were used to show that the improvement in BA and diminished food effect of the nanosized aprepitant formulation in the fasted state is due to its extremely high dissolution rate. Model-4 incorporates a partial restriction into the membrane permeability as well as z values calculated in accordance with the lower particle size in the nanosized formulation. Simulations with Model-4 accurately reflected the dependency of the absorption of aprepitant on the administered dose and its particle size. Thus, the IVISIV-R approach may be a helpful tool in the development of nanosized formulations aiming to achieve the twin goals of enhancement of absorption and elimination of the food effect for poorly soluble drugs.

References

[1] Y. Wu, A. Loper, E. Landis, L. Hettrick, L. Novak, K. Lynn, C. Chen, K. Thompson, R. Higgins, U. Batra, S. Shelukar, G. Kwei, D. Storey, The role of biopharmaceutics in the development of a clinical nanoparticle formulation of MK-0869: a Beagle dog model predicts improved bioavailability and diminished food effect on absorption in human, Int. J. Pharm. 285 (2004) 135–146.
[2] US FDA. Guidance for Industry: Waiver of *in vivo* bioavailability and bioequivalence studies for immediate-release solid oral dosage forms based on a biopharmaceutics classification system, 2000.
[3] R. Löbenberg, G.L. Amidon, Modern bioavailability, bioequivalence and biopharmaceutics classification system. New scientific approaches to international regulatory standards, Eur. J. Pharm. Biopharm. 50 (2000) 3–12.
[4] D. Fleisher, C. Li, Y. Zhou, L.H. Pao, A. Karim, Drug, meal and formulation interactions influencing drug absorption after oral administration. Clinical implications, Clin. Pharmacokinet. 36 (1999) 233–254.
[5] B.N. Singh, Effects of food on clinical pharmacokinetics, Clin. Pharmacokinet. 37 (1999) 213–255.
[6] US FDA. Guidance for Industry: Food-effect bioavailability and fed bioequivalence studies, 2002.

[7] B. Kaeser, J.E. Charoin, M. Gerber, P. Oxley, H. Birnboeck, N. Saiedabadi, L. Banken, Assessment of the bioequivalence of two nelfinavir tablet formulations under fed and fasted conditions in healthy subjects, Int. J. Clin. Pharmacol. Ther. 43 (2005) 154–162.
[8] S. Noble, D. Faulds, Saquinavir. A review of its pharmacology and clinical potential in the management of HIV infection, Drugs 52 (1996) 93–112.
[9] S.C. Sweetman (Ed.), Martindale: The Complete Drug Reference, Pharmaceutical Press, London, Chicago, 2009.
[10] S. Stegemann, F. Leveiller, D. Franchi, H. de Jong, H. Linden, When poor solubility becomes an issue: from early stage to proof of concept, Eur. J. Pharm. Sci. 31 (2007) 249–261.
[11] A.T. Serajuddin, Salt formation to improve drug solubility, Adv. Drug. Deliv. Rev. 59 (2007) 603–616.
[12] N. Blagden, M. de Matas, P.T. Gavan, P. York, Crystal engineering of active pharmaceutical ingredients to improve solubility and dissolution rates, Adv. Drug. Deliv. Rev. 59 (2007) 617–630.
[13] F. Kesisoglou, S. Panmai, Y. Wu, Nanosizing-oral formulation development and biopharmaceutical evaluation, Adv. Drug. Deliv. Rev. 59 (2007) 631–644.
[14] D.J. Hauss, Oral lipid-based formulations, Adv. Drug. Deliv. Rev. 59 (2007) 667–676.
[15] E. Merisko-Liversidge, G.G. Liversidge, E.R. Cooper, Nanosizing: a formulation approach for poorly-water-soluble compounds, Eur. J. Pharm. Sci. 18 (2003) 113–120.
[16] S. Maciejewski, D. Hilleman, Effectiveness of a fenofibrate 145-mg nanoparticle tablet formulation compared with the standard 160-mg tablet in patients with coronary heart disease and dyslipidemia, Pharmacotherapy 28 (2008) 570–575.
[17] K.A. Lentz, Current methods for predicting human food effect, AAPS J. 10 (2008) 282–288.
[18] J.M. Custodio, C.Y. Wu, L.Z. Benet, Predicting drug disposition, absorption/elimination/transporter interplay and the role of food on drug absorption, Adv. Drug. Deliv. Rev. 60 (2008) 717–733.
[19] C.H. Gu, H. Li, J. Levons, K. Lentz, R.B. Gandhi, K. Raghavan, R.L. Smith, Predicting effect of food on extent of drug absorption based on physicochemical properties, Pharm. Res. 24 (2007) 1118–1130.
[20] J.B. Dressman, G.L. Amidon, C. Reppas, V.P. Shah, Dissolution testing as a prognostic tool for oral drug absorption: immediate release dosage forms, Pharm. Res. 15 (1998) 11–22.
[21] E. Jantratid, N. Janssen, H. Chokshi, K. Tang, J.B. Dressman, Designing biorelevant dissolution tests for lipid formulations: case example – lipid suspension of RZ-50, Eur. J. Pharm. Biopharm. 69 (2008) 776–785.
[22] V.H. Sunesen, B.L. Pedersen, H.G. Kristensen, A. Mullertz, In vivo in vitro correlations for a poorly soluble drug, danazol, using the flow-through dissolution method with biorelevant dissolution media, Eur. J. Pharm. Sci. 24 (2005) 305–313.
[23] J.B. Dressman, K. Thelen, E. Jantratid, Towards quantitative prediction of oral drug absorption, Clin. Pharmacokinet. 47 (2008) 655–667.
[24] N. Parrott, T. Lave, Prediction of intestinal absorption: comparative assessment of GASTROPLUS and IDEA, Eur. J. Pharm. Sci. 17 (2002) 51–61.
[25] S. Willmann, J. Lippert, W. Schmitt, From physicochemistry to absorption and distribution: predictive mechanistic modelling and computational tools, Expert Opin. Drug. Metab. Toxicol. 1 (2005) 159–168.
[26] E. Nicolaides, E. Galia, C. Efthymiopoulos, J.B. Dressman, C. Reppas, Forecasting the in vivo performance of four low solubility drugs from their in vitro dissolution data, Pharm. Res. 16 (1999) 1876–1882.
[27] E. Nicolaides, M. Symillides, J.B. Dressman, C. Reppas, Biorelevant dissolution testing to predict the plasma profile of lipophilic drugs after oral administration, Pharm. Res. 18 (2001) 380–388.
[28] S.K. Paulson, J.D. Hribar, N.W. Liu, E. Hajdu, R.H. Bible Jr., A. Piergies, A. Karim, Metabolism and excretion of [(14)C]celecoxib in healthy male volunteers, Drug. Metab. Dispos. 28 (2000) 308–314.
[29] Y. Shono, E. Jantratid, N. Janssen, F. Kesisoglou, Y. Mao, M. Vertzoni, C. Reppas, J.B. Dressman, Prediction of food effects on the absorption of celecoxib based on biorelevant dissolution testing coupled with physiologically based pharmacokinetic modeling, Eur. J. Pharm. Biopharm. 73 (2009) 107–114.
[30] E. Galia, E. Nicolaides, D. Hörter, R. Löbenberg, C. Reppas, J.B. Dressman, Evaluation of various dissolution media for predicting *in vivo* performance of class I and II drugs, Pharm. Res. 15 (1998) 698–705.
[31] M. Vertzoni, J. Dressman, J. Butler, J. Hempenstall, C. Reppas, Simulation of fasting gastric conditions and its importance for the in vivo dissolution of lipophilic compounds, Eur. J. Pharm. Biopharm. 60 (2005) 413–417.
[32] E. Jantratid, N. Janssen, C. Reppas, J.B. Dressman, Dissolution media simulating conditions in the proximal human gastrointestinal tract: an update, Pharm. Res. 25 (2008) 1663–1676.
[33] S. Klein, The mini paddle apparatus-a useful tool in the early developmental stage? Experiences with immediate-release dosage forms, Dissol. Technol. 13 (4) (2006) 6–11.
[34] A.K. Majumdar, L. Howard, M.R. Goldberg, L. Hickey, M. Constanzer, P.L. Rothenberg, T.M. Crumley, D. Panebianco, T.E. Bradstreet, A.J. Bergman, S.A. Waldman, H.E. Greenberg, K. Butler, A. Knops, I. De Lepeleire, N. Michiels, K.J. Petty, Pharmacokinetics of aprepitant after single and multiple oral doses in healthy volunteers, J. Clin. Pharmacol. 46 (2006) 291–300.
[35] P. Macheras, C. Reppas, J.B. Dressman, Biopharmaceutics of Orally Administered Drugs, Ellis Horwood Ltd., London, 1995.
[36] R. Takano, K. Sugano, A. Higashida, Y. Hayashi, M. Machida, Y. Aso, S. Yamashita, Oral absorption of poorly water-soluble drugs: computer simulation of fraction absorbed in humans from a miniscale dissolution test, Pharm. Res. 23 (2006) 1144–1156.
[37] R. Takano, K. Furumoto, K. Shiraki, N. Takata, Y. Hayashi, Y. Aso, S. Yamashita, Rate-limiting steps of oral absorption for poorly water-soluble drugs in dogs; prediction from a miniscale dissolution test and a physiologically-based computer simulation, Pharm. Res. 25 (10) (2008) 2334–2344.
[38] S.C. Sutton, Role of physiological intestinal water in oral absorption, AAPS J. 11 (2) (2009) 277–285.
[39] N. Fotaki, M. Symillides, C. Reppas, In vitro versus canine data for predicting input profiles of isosorbide-5-mononitrate from oral extended release products on a confidence interval basis, Eur. J. Pharm. Sci. 24 (1) (2005) 115–122.
[40] L.X. Yu, An integrated model for determining causes of poor oral drug absorption, Pharml. Res. 16 (12) (1999) 1883–1887.
[41] S. Willmann, W. Schmitt, J. Keldenich, J. Lippert, J.B. Dressman, A physiological model for the estimation of the fraction dose absorbed in humans, J. Med. Chem. 47 (16) (2004) 4022–4031.
[42] J.B. Dressman, C. Reppas, In vitro–in vivo correlations for lipophilic, poorly water-soluble drugs, Eur. J. Pharm. Sci. 11 (Suppl. 2) (2000) S73–S80.
[43] R.H. Müller, K. Peters, Nanosuspensions for the formulation of poorly soluble drugs: I. Preparation by a size-reduction technique, Int. J. Pharm. 160 (1998) 229–237.
[44] W. Wu, G.H. Nancollas, A new understanding of the relationship between solubility and particle size, J. Solution Chem. 27 (6) (1998) 521–531.
[45] A. Godec, M. Gaberscek, J. Jamnik, Comment on the article a new understanding of the relationship between solubility and particle size by W. Wu and G.H. Nancollas, J. Solution Chem. 38 (1) (2009) 135–146.
[46] G.H. Nancollas, W. Wu, Response to comment on a new understanding of the relationship between solubility and particle size by A. Godec, J. Jamnik and M. Gaderscek, J. Solution Chem. 38 (1) (2009) 147–148.
[47] L.X. Yu, G.L. Amidon, A compartmental absorption and transit model for estimating oral drug absorption, Int. J. Pharm. 186 (2) (1999) 119–125.
[48] L. Kalantzi, K. Goumas, V. Kalioras, B. Abrahamsson, J.B. Dressman, C. Reppas, Characterization of the human upper gastrointestinal contents under conditions simulating bioavailability/bioequivalence studies, Pharm. Res. 23 (2006) 165–176.